Temperature-Sensitive, Fluorescent Poly(*N*-Isopropyl-acrylamide)-Grafted Cellulose Nanocrystals for Drug Release

Weibing Wu,[a,b] Jian Li,[a] Wei Liu,[b] and Yulin Deng [b,*]

Cellulose nanocrystals (CNCs) grafted with fluorescent and thermo-responsive poly (*N*-isopropylacryalamide) (PNIPAM) brushes were prepared for encapsulation and the release of 5-fluorouracil (5-FU). The successful grafting was evidenced by Fourier transform infrared (FTIR) spectroscopy and solid-state 13C nuclear magnetic resonance (^{13}C NMR). Differential scanning calorimetry measurements suggested that the lower critical solution temperature of PNIPAM-grafted CNCs is close 32 °C. During polymerization, tuned fluorescence signatures were obtained by varying the dye dosages. At room temperature, the release amount of the loaded 5-FU was about 42% at a pH of 2.1, while this value approached 60% at a pH of 7.4. Both the cumulative release amount and the release rate were greatly increased when the temperature was raised to 37 °C. The novel PNIPAM-grafted CNCs with both fluorescence and stimuli-sensitive properties possess potential for application in intelligent drug delivery systems.

Keywords: Cellulose nanocrystals; Poly (N-isopropylacryalamide); Thermo-sensitivity; Fluorescence; Drug release

Contact information: a: Jiangsu Provincial Key Lab of Pulp and Paper Science and Technology, Jiangsu Co-Innovation Center for Efficient Processing and Utilization of Forest Resources, Nanjing Forestry University, Nanjing, 210037, China; b: School of Chemical & Biomolecular Engineering and RBI at Georgia Tech, Georgia Institute of Technology, 500 10th Street N. W., Atlanta, GA 30332, USA;
** Corresponding author: yulin.deng@rbi.gatech.edu*

INTRODUCTION

Drug-loaded nano-carriers have attracted great interest in the area of delivery and targeting of therapeutic medicine. Nano-sized particles overcome biological barriers to arrive at the target organs and avoid rapid clearance by phagocytes, which greatly prolong their duration in the bloodstream (Langer and Tirrell 2004; Alexis *et al.* 2008; Liu *et al.* 2008; Slowing *et al.* 2008; Wang *et al.* 2009). Various nanoparticle-based technologies have been investigated and applied in clinical use, such as liposomal formulations for cancer therapy, colloidal gold for *in vitro* diagnostics, magnetic nanoparticles for *in vivo* imaging, and polymeric micelles and nanogels for drug delivery (Das *et al.* 2005; Wagner *et al.* 2006; Oh *et al.* 2008; Han *et al.* 2012; Su *et al.* 2013). Among these nanomaterials, cellulose nanocrystals (CNCs) have important application prospects. CNCs are typically produced after acid hydrolysis of crystalline cellulose, and they are rod-like particles 100 nm to 300 nm in length and 5 nm to 15 nm in width (Habibi *et al.* 2010). They possess the advantages of high abundance, low cost, renewability, biodegradability, and reactive surface groups for chemical modification.

Recently, stimuli-responsive nanoparticles have been extensively investigated and applied with the drug delivery system (Rejinold *et al.* 2011a; Zhang *et al.* 2012; Rejinold *et al.* 2014). Most of the smart polymers are environmentally responsive, including poly-(methacrylic acid), poly-(4-vinylpyridine) (Kan *et al.* 2013), poly-(*N*-isopropyl-acrylamide) (Zoppe *et al.* 2010), poly-(*N,N*-dimethylaminoethyl methacrylate) (Yi *et al.* 2009), poly-(2-hydroxyethyl methacrylate), and poly-(ethylene glycol) methacrylates (Porsch *et al.* 2011). Of these smart materials, temperature-responsive poly-(*N*-isopropyl acrylamide) PNIPAM has been widely studied and applied (Binkert *et al.* 1991; O'Shea *et al.* 2011). It exhibits lower critical solution temperatures (LCST) in the range of 32 °C to 33 °C, depending on the detailed microstructure of the macromolecules. Thermo-responsive CNCs were previously synthesized with PNIPAM brushes *via* the surface grafting method (Wu *et al.* 2015). With the immobilization of the CNC core, the grafted PNIPAM brushes behave like a sensitive nanogel (Su *et al.* 2013; Rejinold *et al.* 2014; Zhang *et al.* 2014). Unlike bulk hydrogel or a microgel with poor mechanical strength (Ghugare *et al.* 2009; Hebeish *et al.* 2014), the rigid CNC core provides the stability and mechanical strength. Moreover, since cellular uptake and the biodistribution of nanoparticulate delivery systems can be studied using fluorescence techniques, multifunctional nanocarriers combining imaging function with drug delivery are emerging as the next generation of nanomedicines to improve the outcome of drug therapy (Bryl and Langner 2005). When fluorescent and thermo-responsive CNCs were used as the carriers for drug delivery, the fluorescence made it possible to observe the distribution of the drug-loaded CNCs and monitor the drug release dynamic process in the tissues and organs. 5-Fluorocuracil (5-FU) is a widely used anticancer drug. Its acylamino group and limited solubility in water make it possible to effectively load 5-FU in the surface-grafted thermo-responsive CNCs via hydrogen bonding (Zhang *et al.* 2012). The aim of this study was to investigate the thermo-responsiveness, fluorescent properties, and drug release behaviors of the polymer-grafted CNCs under different conditions.

EXPERIMENTAL

Materials

N-isopropylacryalamide (NIPAM, 97%) and phosphate buffer, with a pH of 2.1 and 7.4, were obtained from VWR (USA). Copper(II) bromide ($CuBr_2$, 99%), 4-bromo-1,8-naphthalic anhydride (95%), 2-bromoisobutyryl bromide (BiB, 98%), L-ascorbic acid (AsAc, 99%), *N,N,N′,N″,N‴*-pentamethyldiethylenetriamine (PMDETA, 99%), 2-dimethylaminopyridine (DMAP, 99%), 5-FU, allylamine (99%), acetone (99.8%), tetrahydrofuran (THF, 99.9%), ethanol (99.5%), and methanol (CH_3OH, 99.8%) were all purchased from Sigma-Aldrich (USA). All chemicals were used as they were received without purification. The reagents 4-ethoxy-9-allyl-1, 8-naphthalimide (EANI), and 4-methylamino-9-allyl-1,8-naphthalimide (MANI) were synthesized as described (Grabchev and Konstantinova 1997; Grabtchev *et al.* 1997).

Synthesis of CNCs Grafted with Copolymer Brushes (CNCs-GF)

The procedure to prepare CNCs and initiator-immobilized CNCs (CNCs-Br) was described previously (Wu *et al.* 2015). The typical synthesis procedure of CNCs-GF uses

activators generated by an electron transfer for atom transfer radical polymerization (AGET-ATRP). In this procedure, 0.15 g of initiator-immobilized CNCs (CNCs-Br), 3.39 g of NIPAM (30.0 mmol), 67 mg of $CuBr_2$ (0.3 mmol), 125 μL of PMDETA (0.3 mmol), EANI, and MANI in 11.25 mL of a CH_3OH/H_2O mixture (volume ratio of 1:1) was added to a Schlenk tube under magnetic stirring, and the mixture was bubbled with nitrogen for 20 min. Another Schlenk tube containing 26 mg of AsAc (0.15 mmol) in 3.75 mL of a CH_3OH/H_2O mixture (volume ratio of 1:1) was bubbled with nitrogen for 15 min. Afterwards, the degassed AsAc solution was transferred to the first Schlenk tube. The tube was sealed with a rubber septum and kept at ambient temperature for 8 h. The polymerization was quenched by exposure to air. The reaction mixture was centrifuged for 20 min at 12,000 rpm at 4 °C. Successive washing with acetone, DI water, and methanol purified the isolated precipitates. The samples named CNCs-GF1, CNCs-GF2, CNCs-GF3, CNCs-GF4, CNCs-GF5, and CNCs-GF6 were generated with the EANI/MANI ratios of 10:0, 6:4, 5:5, 4:6, 2:8, and 0:10, respectively. The total amount of EANI and MANI was fixed at 0.4 mmol.

Preparation of 5-FU-Loaded CNCs-GF

The drug loading was conducted using CNCs-GF3 as the carrier and 5-FU as the model drug. Briefly, 5 mg of 5-FU was dissolved in 20 mL of CNCs-GF3 solution (0.25 wt.%). After incubation in a 25 °C water bath for 12 h and subsequently in a 37 °C water bath for 12 h, the solution was centrifuged at 10,000 rpm for 10 min at 4 °C. The collected precipitates were purified by centrifugation and washed with DI water to remove the non-encapsulated drug. The precipitates were freeze-dried and kept in a vacuum desiccator. The concentration of 5-FU in the washing solution was analyzed by UV absorbance at the wavelength of 266 nm, with respect to the standard calibration curve. The drug-loaded content (η) of CNCs-GF3 was calculated as follows,

$$\eta = \frac{m_0 - C_D V}{m + m_0 - C_D V} \times 100\% \quad (1)$$

where m_0 is the drug dosage, m is the weight of CNCs-GF3, C_D is the concentration of 5-FU in the washing solution, and V is the total volume of washing solution.

Drug Release Experiment

Fifty mg above the amount of 5-FU-loaded CNCs-GF3 (5-FU@CNCs-GF3) were dispersed in 20 mL of the phosphate buffer solution and transferred to a dialysis membrane bag (MWCO 3.5 kDa). The membrane was then immersed in 200 mL of the phosphate buffer solution at a designated temperature of 25 or 37 °C, and pH of 2.1 or 7.4. A 2 mL aliquot of release medium was periodically taken out from the system for analysis, and then 2 mL of fresh buffer solution was added back into the release system. The concentration of 5-FU in each aliquot was measured by a UV spectrophotometer, and the amount of the released drug was obtained by a comparison with the standard calibration curve. The cumulative drug release (R) was calculated according to Eq. (2). All of the drug-release studies were performed in triplicate and the average value of the three determinations was shown in the data analysis,

$$R = \frac{200\ C_n + 2.0\ \sum C_{n-1}}{m_0 - C_D V} \times 100\% \quad (2)$$

where C_n and C_{n-1} are the concentration of 5-FU at n and n-1 times of drawing out of the buffer solution, respectively.

Methods

Fourier transform infrared (FTIR) spectra were recorded on a FTIR-650 spectrometer (Gangdong Sci. & Tec., Tianjin, China). The transmission electron microscopy (TEM) images were obtained on a JEOL 100CX II transmission electron microscope (Japan) under the acceleration voltage of 80 kV. The solid-state ^{13}C nuclear magnetic resonance (NMR) spectral data were recorded with a Bruker Avance/DMX 400 MHz NMR spectrometer (Swiss) at 25 °C. Differential scanning calorimetry (DSC) measurements were run to measure the phase transition temperatures using 10 mg samples in 20 μL of water in sealed aluminum pans on a TA instruments Q1000 DSC (USA) calibrated with indium. The samples were scanned from 10 °C to 60 °C, at 5 °C/min, under a nitrogen flow of 20 cm^3/min, and referenced against an empty pan. The fluorescence measurements were conducted on a Shimadzu RF-5301PC (Japan) equipped with a xenon lamp. The widths of the excitation and emission slit were 5.0 mm.

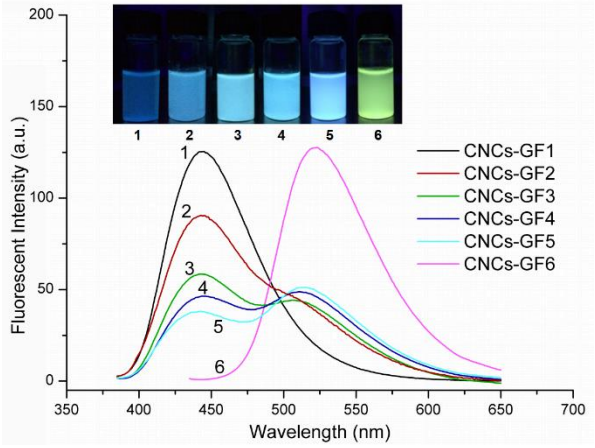

Fig. 1. The fluorescence emission spectroscopy of CNCs-GF (0.02 wt.% in H_2O) under 375-nm excitation. CNCs-GF6 was solely excited at 425 nm; the top photograph of CNCs-GF suspensions (0.05 wt.%) was taken under 365-nm UV illumination.

RESULTS AND DISCUSSION

Fluorescent Properties of CNCs-GF

The chemical structures of CNCs and modified CNCs were identified by FTIR (Fig. S1), and solid-state ^{13}C NMR (Fig. S2). A series of CNCs-GF populations with different fluorescence signatures was obtained by changing the dosages of dyes during the polymerization (Fig. 1). The CNCs labeled with only one dye showed typical single-peak emissions, which were almost the same as those of pure dye solutions, such as CNCs-GF1 (EANI only) and CNCs-GF6 (MANI only). However, the CNCs-GF labeled with both EANI and MANI had two emission peaks at 444 nm and 522 nm. Fluorescence resonance energy transfer (FRET) occurs between EANI and MANI groups when they are simultaneously encapsulated into polystyrene microspheres (Wu *et al.* 2008). Based on the

similar fluorescent features of the CNCs-GF series, FRET may have contributed to the dual emission signals from CNCs-GF2 to CNCs-GF5. As shown in the inset picture in Fig. 1 (365-nm UV illumination), the CNCs-GF suspensions displayed different colors corresponding to their emission spectrum. More CNCs-GF populations with tunable and distinguishable fluorescent signals can be obtained by varying the fluorescent intensity and the intensity ratio of two peaks.

Thermo-Responsiveness of CNCs-GF

The polymer PNIPAM is a well-known temperature-sensitive polymer with a lower critical solution temperature (LCST) at 32 °C, which is slightly lower than the average body temperature. PNIPAM undergoes a coil-to-globule transition when the temperature is higher than the LCST (Masci *et al.* 2004; Ifuku and Kadla 2008). The CNCs-GF is not soluble in water, but the suspension appears almost clear at room temperature. The stabilized dispersion system is attributed to the hydrophilicity of the CNC backbone and the PNIPAM side-chain. When the temperature of the suspension was increased to above 35 °C, the solution became cloudy (Fig. 2). This phase transition behavior was reversible. Above the LCST, the grafted PNIPAM side-chain transforms to a hydrophobic globule structure; as a result, the CNCs-GF particles coagulate and precipitate from the solution. The thermal transition property of CNCs-GF was investigated using DSC (Fig. 2). The phase transition peak values for the heating and cooling process were 31.2 °C and 33.1 °C, respectively, which are close to those of the PNIPAM homopolymer.

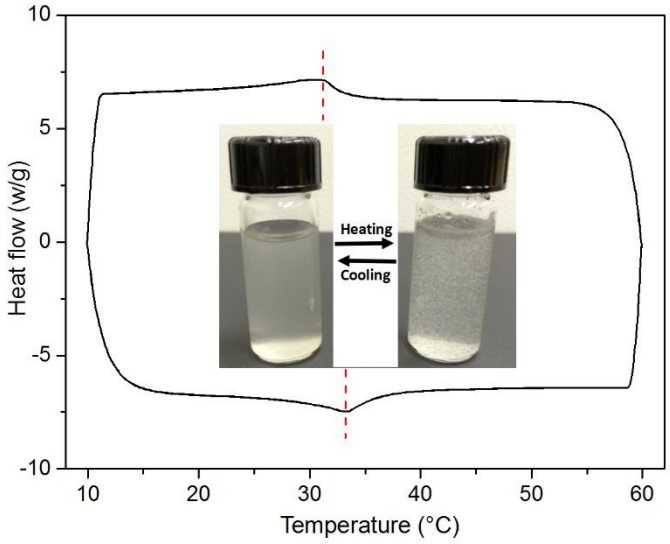

Fig. 2. DSC analysis of CNCs-GF in water (33.3 wt.%). The inset is the visual appearance of the phase transition of CNCs-GF in water

Morphology and Particle Size of CNCs-GF

Figure 3 shows TEM images of CNCs, CNCs-GF3, and 5-FU@CNCs-GF3. The original CNCs were rod-like particles with dimensions of 5 nm to 15 nm in width and 100 nm to 200 nm in length, which are comparable to the reported sizes of CNCs (Roman and Winter 2004). After the surface grafting, the length of CNCs-GF3 generally remained the same, but the width was increased to 30 nm to 50 nm. The coarse morphology indicates

the presence of the grafted polymer brushes on the surface of the CNCs. The 5-FU@CNCs-GF3 had a similar morphology and particle size (Fig. 3C).

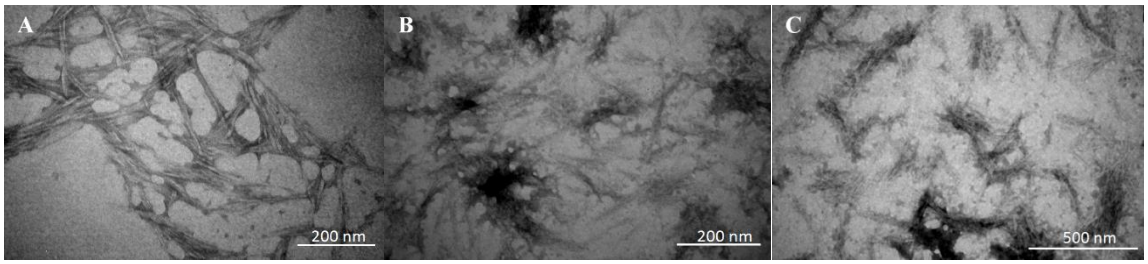

Fig. 3. TEM images of CNCs (A), CNCs-GF (B), and 5-FU@CNCs-GF3 (C)

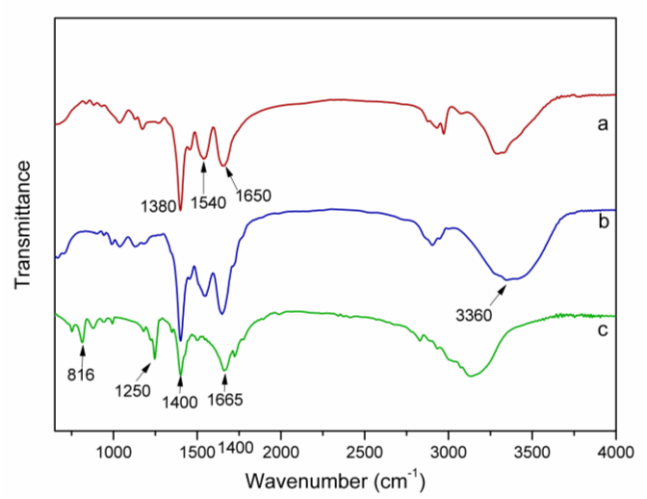

Fig. 4. FTIR spectra of CNCs-GF3 (a), 5-FU@CNCs-GF3 (b), and 5-FU (c)

5-FU Loading in CNCs-GF

The entrapment of 5-FU in CNCs-GF3 and the interactions between them were investigated by FTIR. Figure 4 shows the FTIR spectra of drug 5-FU, surface-grafted CNCs-GF3, and drug-loaded 5-FU@CNCs-GF3. Characteristic absorption bands of 5-FU were clearly apparent at 1665 cm^{-1}, 1400 cm^{-1}, 1250 cm^{-1}, and 816 cm^{-1} (Fig. 4c). Nanoparticles with amino or hydroxyl groups on their chains increase the drug-loading capacity, due to the hydrogen bonding for 5-FU containing electronegative atoms (Zhang *et al.* 2012). Compared with the spectrum of CNCs-GF3 (Fig. 4a), the absorption band 5-FU@CNCs-GF3 (Fig. 4b) at 3360 cm^{-1} became much stronger, supporting the existence of hydrogen bonding between CNCs-GF3 and 5-FU (Rejinold *et al.* 2011b).

After drug loading, the characteristic absorption bands at 1250 cm^{-1} and 816 cm^{-1} of 5-FU were not observed for 5-FU@CNCs-GF3. The disappearance of absorption bands can also be attributed to hydrogen bonding and van der Waals interaction between 5-FU and CNCs-GF3. Obviously, the existence of interaction between drug and carrier is beneficial to drug loading. The final 5-FU-loading content was about 2 wt.%, as calculated by Eq. (1).

Release of 5-Fu from CNCs-GF

The cumulative release of 5-FU@CNCs-GF3 during 10 h under different conditions is shown in Figure 5. 5-FU@CNCs-GF3 showed faster release rates during the initial time but slower rates at the later stage. The acceleration of the drug release at the earlier stage was attributed to the big difference of concentration around CNCs-GF3. Rapid drug release would help reach the drug concentration required for the clinical treatment in a short time. At the later stage, the moderate drug release, which was slowed down by the hydrogen bonding interaction between 5-FU and CNCs-GF3, is beneficial to keep the drug concentration stable during clinical treatment.

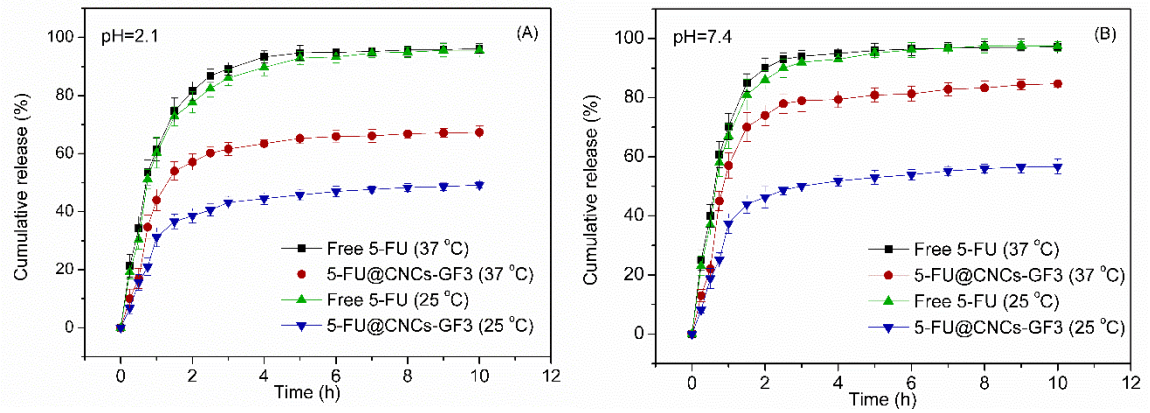

Fig. 5. 5-FU release kinetics of CNCs-GF3 at different conditions during 10 h

The carrier materials remarkably affected the release of 5-FU. Under the same external conditions, the cumulative release amount of 5-FU@CNCs-GF3 was dramatically decreased compared with that of free 5-FU. The temperature and pH also were important to the cumulative release amount. At a pH of 7.4, the cumulative amount released of 5-FU from CNCs-GF3 increased from 50% to 80%, when temperature was changed from 25 °C to 37 °C. As the temperature increased, the grafted PNIPAM brushes become hydrophobic above the LCST and formed a shrinking state of polymer chains, which promoted the release of 5-FU.

Meanwhile, the increase in temperature weakened the hydrogen bonding between 5-FU and CNCs-GF3, hence accelerating the drug release rate. In contrast, hydrogen bonding was capable of holding drugs in the carrier below the LCST. A certain amount of 5-FU still remained in CNCs-GF3, which may be due to the highly hydrated PNIPAM chains stabilizing the drug that was loaded.

The above results demonstrated that PNIPAM-grafted CNCs had a good temperature-controlled drug release behavior. Figure 5 also reveals that the medium pH affected the release kinetics of 5-FU@CNCs-GF3. At a pH of 2.1, the cumulative releases of 5-FU were 42% at 25 °C and 62% at 37 °C, both of which were remarkably reduced compared with those in pH 7.4. Given that the pH value influenced the solubility of 5-FU, the less cumulative drug release was attributed to the lower solubility of 5-FU in an acidic medium.

CONCLUSIONS

1. CNCs grafted with fluorescent and thermo-responsive PNIPAM brushes were prepared, and the chemical structure was confirmed by FTIR and solid-state ^{13}C NMR.
2. DSC showed that the LCST of PNIPAM-grafted CNCs was close to 32 °C. The fluorescent signals of the PNIPAM-grafted CNCs could be tuned by varying the dye concentrations.
3. The 5-FU was successfully encapsulated into the PNIPAM-grafted CNCs *via* the hydrogen bonding. Increasing the temperature or the pH of the solutions accelerated the release of 5-FU from the PNIPAM-grafted CNCs. The environmentally sensitive properties of PNIPAM-grafted CNCs make them feasible for controlling drug release by alternating the external conditions.

ACKNOWLEDGMENTS

This work was supported by the National Natural Science Foundation of China (No. 31200453) and the Priority Academic Program Development of Jiangsu Higher Education Institutions (PAPD).

REFERENCES CITED

Alexis, F., Pridgen, E., Molnar, L. K., and Farokhzad, O. C. (2008). "Factors affecting the clearance and biodistribution of polymeric nanoparticles," *Mol. Pharmaceut.* 5(4), 505-515. DOI: 10.1021/mp800051m

Binkert, T., Oberreich, J., Meewes, M., Nyffenegger, R., and Ricka, J. (1991). "Coil-globule transition of poly(N-isopropylacrylamide): A study of segment mobility by fluorescence depolarization," *Macromolecules* 24(21), 5806-5810. DOI: 10.1021/ma00021a013

Bryl, K., and Langner, M. (2005). "Fluorescence applications in targeted drug delivery," in: *Fluorescence Spectroscopy in Biology: Advanced Methods and their Applications to Membranes, Proteins, DNA, and Cells*, M. Hof, R. Hutterer, and V. Fidler (eds.), Springer, New York, USA, pp. 229-242.

Das, M., Mardyani, S., Chan, W., and Kumacheva, E. (2005). "Biofunctionalized pH-responsive microgels for cancer cell targeting: Rational design," *Adv. Mater.* 18(1), 80-83. DOI: 10.1002/adma.200501043

Grabchev, I., and Konstantinova, T. (1997). "Synthesis of some polymerisable 1, 8-naphthalimide derivatives for use as fluorescent brighteners," *Dyes Pigments* 33(3), 197-203. DOI: 10.1016/S0143-7208(96)00053-8

Grabtchev, I., Konstantinov, T., Guittonneau, S., and Meallier, P. (1997). "Photochemistry of some 1, 8-naphthalic anhydride derivatives," *Dyes Pigments* 35(4), 361-366. DOI: 10.1016/S0143-7208(96)00116-7

Habibi, Y., Lucia, L. A., and Rojas, O. J. (2010). "Cellulose nanocrystals: Chemistry, self-assembly, and applications," *Chem. Rev.* 110(6), 3479-3500. DOI: 10.1021/cr900339w

Han, S., Liu, Y., Nie, X., Xu, Q., Jiao, F., Li, W., Zhao, Y., Wu, Y., and Chen, Y. (2012). "Efficient delivery of antitumor drug to the nuclei of tumor cells by amphiphilic biodegradable poly (L-aspartic acid-co-lactic acid)/DPPE co-polymer nanoparticles," *Small* 8(10), 1596-1606. DOI: 10.1002/smll.201102280

Hebeish, A., Farag, S., Sharaf, S., and Shaheen, T. I. (2014). "Thermal responsive hydrogels based on semi interpenetrating network of poly (NIPAm) and cellulose nanowhiskers," *Carbohyd. Polym.* 102, 159-166. DOI: 10.1016/j.carbpol.2013.10.054

Ifuku, S., and Kadla, J. F. (2008). "Preparation of a thermosensitive highly regioselective cellulose/N-isopropylacrylamide copolymer through atom transfer radical polymerization," *Biomacromolecules* 9(11), 3308-3313. DOI: 10.1021/bm800911w

Kan, K. H., Li, J., Wijesekera, K., and Cranston, E. D. (2013). "Polymer-grafted cellulose nanocrystals as pH-responsive reversible flocculants," *Biomacromolecules* 14(9), 3130-3139. DOI: 10.1021/bm400752k

Langer, R., and Tirrell, D. A. (2004). "Designing materials for biology and medicine," *Nature* 428(6982), 487-492. DOI: 10.1038/nature02388

Liu, Z., Jiao, Y., Wang, Y., Zhou, C., and Zhang, Z. (2008). "Polysaccharides-based nanoparticles as drug delivery systems," *Adv. Drug. Delivery Rev.* 60(15), 1650-1662. DOI: 10.1016/j.addr.2008.09.001

Masci, G., Giacomelli, L., and Crescenzi, V. (2004). "Atom transfer radical polymerization of *N*-Isopropylacrylamide," *Macromol. Rapid Comm.* 25(4), 559-564. DOI: 10.1002/marc.200300140

Oh, J. K., Drumright, R., Siegwart, D. J., and Matyjaszewski, K. (2008). "The development of microgels/nanogels for drug delivery applications," *Prog. Polym. Sci.* 33(4), 448-477. DOI: 10.1016/j.progpolymsci.2008.01.002

O'Shea, J.-P., Qiao, G. G., and Franks, G. V. (2011). "Temperature responsive flocculation and solid-liquid separations with charged random copolymers of poly (N-isopropyl acrylamide)," *J. Colloid Interf. Sci.* 360(1), 61-70. DOI: 10.1016/j.jcis.2011.04.013

Porsch, C., Hansson, S., Nordgren, N., and Malmstrom, E. (2011). "Thermo-responsive cellulose-based architectures: Tailoring LCST using poly (ethylene glycol) methacrylates," *Polym. Chem.* 2 (5), 1114-1123. DOI: 10.1039/C0PY00417K

Rejinold, N. S., Baby, T., Chennazhi, K. P., and Jayakumar, R. (2014). "Dual drug encapsulated thermo-sensitive fibrinogen-graft-poly (N-isopropyl acrylamide) nanogels for breast cancer therapy," *Colloid Surface B* 114, 209-217. DOI: 10.1016/j.colsurfb.2013.10.015

Rejinold, N. S., Muthunarayanan, M., Divyarani, V. V., Sreerekha, P. R., Chennazhi, K. P., Nair, S. V., Tamura, H., and Jayakumar, R. (2011a). "Curcumin-loaded biocompatible thermoresponsive polymeric nanoparticles for cancer drug delivery," *J. Colloid Interf. Sci.* 360(1), 39-51. DOI: 10.1016/j.jcis.2011.04.006

Rejinold, N. S., Chennazhi, K. P., Nair, S. V., Tamura, H., and Jayakumar, R. (2011b). "Biodegradable and thermo-sensitive chitosan-g-poly (N-vinylcaprolactam) nanoparticles as a 5-fluorouracil carrier," *Carbohyd. Polym.* 83, 776-786. DOI:10.1016/j.carbpol.2010.08.052

Roman, M., and Winter, W. T. (2004). "Effect of sulfate groups from sulfuric acid hydrolysis on the thermal degradation behavior of bacterial cellulose," *Biomacromolecules* 5(5), 1671-1677. DOI: 10.1021/bm034519+

Slowing, I. I., Vivero-Escoto, J. L., Wu, C. W., and Lin, V. S. Y. (2008). "Mesoporous silica nanoparticles as controlled release drug delivery and gene transfection carriers," *Adv. Drug. Delivery Rev.* 60(11), 1278-1288. DOI: 10.1016/j.addr.2008.03.012

Su, S., Wang, H., Liu, X., Wu, Y., and Nie, G. (2013). "IRGD-coupled responsive fluorescent nanogel for targeted drug delivery," *Biomaterials*, 34(13), 3523-3533. DOI: 10.1016/j.biomaterials.2013.01.083

Wagner, V., Dullaart, A., Bock, A. K., and Zweck, A. (2006). "The emerging nanomedicine landscape," *Nat. Biotechnol.* 24(10), 1211-1217. DOI: 10.1038/nbt1006-1211

Wang, X., Liu, L.-H., Ramström, O., and Yan, M. (2009). "Engineering nanomaterial surfaces for biomedical applications," *Exp. Biol. Med.* 234(10), 1128-1139. DOI: 10.3181/0904-MR-134

Wu, W., Huang, F., Pan, S., Mu, W., Meng, X., Yang, H., Xu, Z., Ragauskas, A. J., and Deng, Y. (2015). "Thermo-responsive and fluorescent cellulose nanocrystals grafted with polymer brushes," *J. Mater. Chem. A* 3(5), 1995-2005. DOI: 10.1039/C4TA04761C

Wu, W.-B., Wang, M.-L., Sun, Y.-M., Huang, W., Cui, Y.-P., and Xu, C.-X. (2008). "Color-tuned FRET polystyrene microspheres by single wavelength excitation," *Opt. Mater.* 30(12), 1803-1809. DOI:10.1016/j.optmat.2007.11.031

Yi, J., Xu, Q., Zhang, X., and Zhang, H. (2009). "Temperature-induced chiral nematic phase changes of suspensions of poly (*N*, *N*-dimethylaminoethyl methacrylate)-grafted cellulose nanocrystals," *Cellulose* 16(6), 989-997. DOI: 10.1007/s10570-009-9350-9

Zhang, L., Wang, L., Guo, B., and Ma, P. X. (2014). "Cytocompatible injectable carboxymethylchitosan/*N*-isopropylacrylamide hydrogels for localized drug delivery," *Carbohyd. Polym.* 103, 110-118. DOI: 10.1016/j.carbpol.2013.12.017

Zhang, T., Li, G., Guo, L., and Chen, H. (2012). "Synthesis of thermo-sensitive CS-g-PNIPAAM/CMC complex nanoparticles for controlled release of 5-FU," *Int. J. Biol. Macromol.* 51(5), 1109-1115. DOI: 10.1016/j.ijbiomac.2012.08.033

Zoppe, J. O., Habibi, Y., Rojas, O. J., Venditti, R. A., Johansson, L. -S., Efimenko, K., Österberg, M., and Laine, J. (2010). "Poly (*N*-isopropylacrylamide) brushes grafted from cellulose nanocrystals *via* surface-initiated single-electron transfer living radical polymerization," *Biomacromolecules* 11(10), 2683-2691. DOI: 10.1021/bm100719d

Article submitted: March 9, 2016; Peer review completed: May 28, 2016; Revised version received: June 22, 2016; Accepted: June 25, 2016; Published: July 11, 2016.
DOI: 10.15376/biores.11.3.7026-7035